



# Synthesis and in vitro evaluation of tetrahydropyridines as potential CDK2 and DprE1 inhibitors

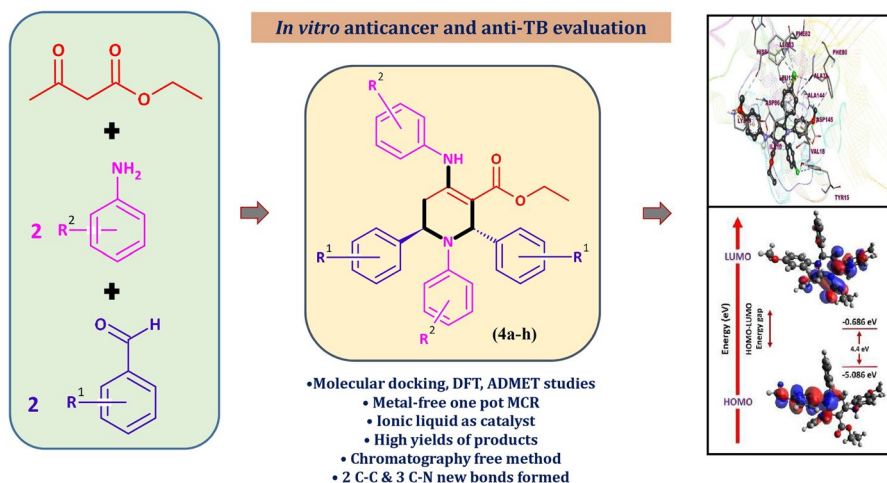
Pravin R. Kharade<sup>1,5</sup> · Uttam B. Chougale<sup>1,5</sup> · Dipak S. Gaikwad<sup>2</sup> ·  
Satish S. Kadam<sup>2</sup> · Kiran N. Patil<sup>3</sup> · Sanket S. Rathod<sup>4</sup> · Prafulla B. Choudhari<sup>4</sup> ·  
Savita S. Desai<sup>5</sup>

Received: 23 November 2023 / Accepted: 8 January 2024  
© The Author(s), under exclusive licence to Springer Nature B.V. 2024

## Abstract

The present work describes the unrevealed potential of tetrahydropyridines as anti-cancer and anti-tubercular agents along with DFT, ADMET, drug-likeness and molecular docking studies synthesized by using Bronsted acidic ionic liquid viz. 1-methyl-3-(4-sulfobutyl)-1H-imidazol-3-ium chloride [MSBIM-Cl]. The synthesized derivatives have been screened for their anticancer and anti-tubercular evaluation against MCF-7 cell lines and Mycobacterium tuberculosis respectively. The compound **4e** showed the highest anticancer activity while the compound **4h** showed the highest anti-tubercular activity. The in vitro evaluation has been supported by computational methods such as molecular docking, density functional study and in silico ADMET and drug-likeness prediction.

## Graphical abstract



Extended author information available on the last page of the article

**Keywords** Tetrahydropyridines · Ionic liquids · Molecular docking · DFT · ADMET

## Introduction

Nitrogen containing heterocyclic compounds plays a vital role in a variety of biomolecules like DNA, RNA, hemoglobin, chlorophyll, vitamins, hormones, amino acids and natural products such as morphine, reserpine, codeine and many more [1–5]. Moreover, N-heterocycles have been utilized to produce drugs, agrochemicals, polymers, dyes and other functional substances [6–12]. In recent years, organic chemists and researchers are found to be interested in synthesis of numerous nitrogen heterocycles as they possess wide range of biological and pharmacological activities [13–18]. Hence the given significance response of N-containing heterocycles as drug molecules in the field of medicinal chemistry, synthesis of newer compounds and modification of existing molecules for better leads found to be a crucial fact in drug discovery [19–23].

During last two decades, organic chemists have been working on sustainable and eco-friendly approaches for the synthesis of heterocyclic compounds [24, 25]. This is prompted by certain disadvantages of the traditional methods like prolonged heating, use of organic solvents and employment of toxic catalysts, among others [26, 27]. So looking towards these facts, an ecofriendly methodology of use of ionic liquids (ILs), in the perspective of green chemistry principles, has gained vital attention of researchers [28–33]. They have been used in organic synthesis, catalysis, electrochemistry, material chemistry, organic synthesis, pretreatment of biomass, separation and analysis [34, 35]. Ionic liquids (ILs) possess unique chemical and physical properties such as thermal stability, non-inflammability, controlled miscibility, low vapor pressure and non-volatility [36, 37]. Furthermore, owing to their high polarity and ability to enhance the rate of reaction, they find extensive use in the synthetic organic chemistry [38–40].

Multi-component reactions (MCRs) have emerged as powerful tool in synthetic organic chemistry because of their ability to generate complex molecules in one step with multiple reactants. Additionally, multi-component tandem reactions provide an easy way to produce desired compounds in two or more steps without extracting the intermediate products. These reactions offer several advantages including waste minimization, absence of side products, minimal reactions times and product purity [41–44].

Naturally occurring alkaloids and related products feature tetrahydropyridine as a basic skeleton [45, 46]. Tetrahydropyridine derivatives exhibit diverse biological activities and therapeutic importance. They have been reported as antimalarial [47], anti-inflammatory [48, 49], anti-hypertensive [50], antibacterial [51], and anticonvulsant [52] etc. So, they are useful in synthetic as well as medicinal fields. The synthesis of tetrahydropyridine derivatives have been achieved by employing variety of catalysts like p-toluene sulfonic acid monohydrate [53], TMSI [54], ruthenium chloride [55], acetic acid [56], tartaric acid [57], citric acid [58], sulfated titania [59], tetrabutylammonium dibromide (TBATB) [60], polystyrene-supported sulfonic acid [61] and many more. However, several of these synthetic approaches

suffer from drawbacks such as long reaction times, high temperatures, use of hazardous solvents, tedious time consuming procedure with low yield of products and high amount of catalysts.

So, under the aspect of green chemistry principles, we synthesized functionalized tetrahydropyridine derivatives using Bronsted acidic ionic liquid as an eco-friendly catalyst in a one-pot multi-component reaction of ethyl acetoacetate, aromatic amines and aromatic aldehydes. This reaction facilitated the formation of five new carbon–carbon bonds. Additionally, we studied the efficacy of the synthesized derivatives against MCF-7 cell lines and Mycobacterium tuberculosis through in-vitro testing of samples. For the first time, the activities of the compounds were supported by molecular docking, DFT, and ADMET prediction alongwith drug-likeness studies.

## Experimental

### Materials and methods

#### General information

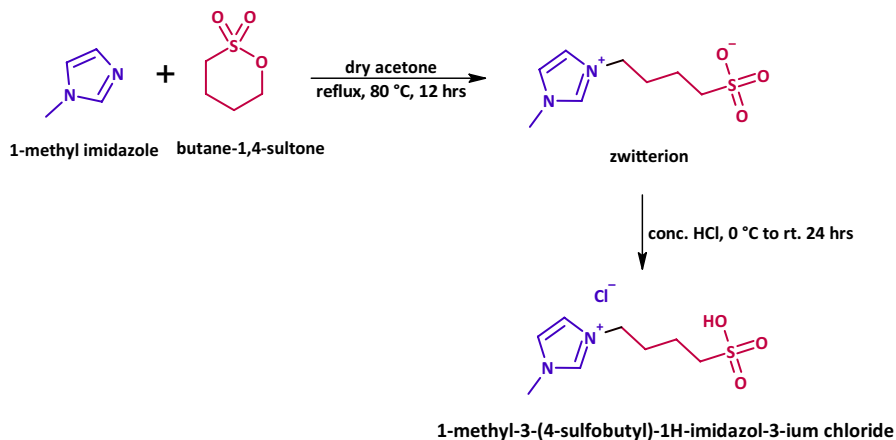
The research grade chemicals were obtained from Aldrich and Spectrochem and used as received. Melting points were determined in open capillaries and were uncorrected. The  $^1\text{H}$  and  $^{13}\text{C}$  NMR spectra were recorded on Bruker spectrometer at 400 and 75 MHz, respectively, using tetramethylsilane (TMS) as an internal standard and  $\text{CDCl}_3$  as solvent. The FT-IR spectra  $\bar{\nu}$  in  $\text{cm}^{-1}$  (KBr) were recorded on Bruker Alpha FT-IR Spectrometer.

#### Preparation of ionic liquid as catalyst

The preparation of ionic liquid was carried out as reported in earlier method with slight modification (Scheme 1) [62]. An equimolar quantity of 1-methylimidazole (10 mmol) and butane-1,4-sultone (10 mmol) was charged into 100 ml round bottle flask containing 50 ml dry acetone at room temperature. Then the reaction mixture was refluxed at 80 °C for 12 h to get zwitterion. Then stoichiometric amount of concentrated HCl (10 mmol) was added dropwise at 0 °C and the resulting reaction mixture was again stirred at room temperature for 24 h to get highly viscous light brown ionic liquid. It was repeatedly washed with acetone and diethyl ether to remove organic impurities. Finally, it was dried in hot air oven for 16 h to get pure ionic liquid.

#### General procedure for the one pot multicomponent synthesis of tetrahydropyridine derivatives (4a-h)

A mixture of ethyl acetoacetate (**1**) (1 mmol), substituted aromatic amines (**2a–d**) (2 mmol), and ionic liquid (IL) 15 mol% in 3 mL ethanol was stirred for one hour at room temperature. Then substituted aldehydes (**3a–d**) (2 mmol) was added to



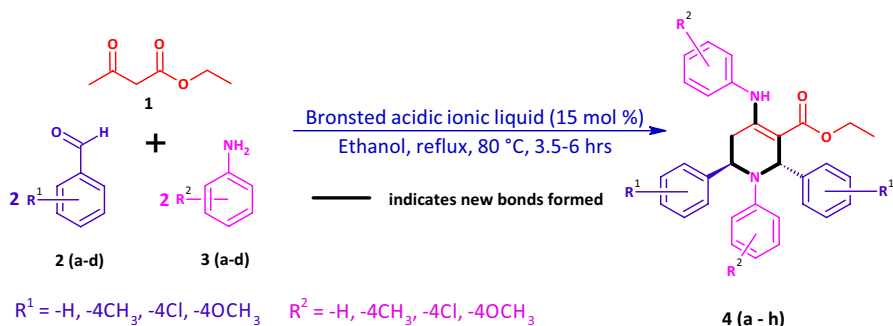
**Scheme 1** Synthesis of ionic liquid catalyst

the above mixture and the reaction mixture then refluxed at 80 °C for 3.5 to 6 h (Scheme 2). After completion of reaction (as indicated by TLC), the reaction mixture was cooled to room temperature and the product formed was filtered at suction, dried and recrystallized from hot ethanol to get pure compound without the use of any column chromatography.

### Spectroscopic data of representative compound 4a.

Ethyl-1-(4-methoxyphenyl)-4-((4-methoxyphenyl)amino)-2,6-diphenyl-1,2,5,6-tetrahydropyridine-3-carboxylate

White Solid, M.P. 170–172 °C, Yield 93%; FT-IR  $\nu_{\text{max}}$   $\text{cm}^{-1}$  (KBr): 3235.81, 3055.90, 2998.34, 2948.23, 2901.85, 2830.11, 1645.59, 1591.90, 1508.09, 1449.77, 1235.51, 1175.50, 1069.72, 1036.34, 958.90, 941.97, 914.00, 845.58, 750.72;  $^1\text{H}$  NMR ( $\text{CDCl}_3$ , 400 MHz):  $\delta$  (ppm) 10.147 (br s, 1H, NH), 7.341–7.266 (m, 6H, ArH), 7.228–7.177 (m, 3H, ArH), 6.681–6.605 (dq, 4H,  $J=12.4$  & 9.2 Hz, ArH), 6.465–6.442 (d, 2H,  $J=9.2$  Hz, ArH), 6.356 (s, 1H, CH-2), 6.213–6.192 (d, 2H,  $J=8.4$  Hz, ArH), 5.066–5.059 (d, 1H,  $J=2.8$  Hz, CH-6), 4.468–4.423 (dd, 1H,



**Scheme 2** Synthesis of tetrahydropyridine derivatives

$J=7.2$  &  $3.6$  Hz,  $\text{OCH}_a\text{CH}_b$ ), 4.336–4.292 (dd, 1H,  $J=6.8$  &  $4.0$  Hz,  $\text{OCH}_a\text{CH}_b$ ), 3.750 (s, 3H,  $\text{ArOCH}_3$ ), 3.667 (s, 3H,  $\text{ArOCH}_3$ ), 2.826–2.774 (dd, 1H,  $J=9.6$  &  $5.6$  Hz,  $\text{CH}_2$ -5), 2.671–2.627 (dd, 1H,  $J=12.8$  &  $2.4$  Hz,  $\text{CH}_2$ -5), 1.470–1.435 (t, 3H,  $J=7.2$  Hz,  $\text{OCH}_2\text{CH}_3$ );  $^{13}\text{C}$  NMR ( $\text{CDCl}_3$ , 75 MHz):  $\delta$  (ppm) 168.33, 157.75, 156.84, 150.86, 144.35, 143.26, 141.56, 130.71, 128.61, 128.14, 127.87, 127.09, 126.80, 126.53, 126.20, 114.48, 114.05, 113.93, 97.20, 59.52, 58.29, 55.63, 55.38, 33.61, 14.81; LC–MS (ESI):  $m/z$  503.35 ( $\text{M} + \text{H}^+$ ).

## Biological activities

### Anticancer activity

The anticancer activity studies have been performed against human breast cancer cell lines (MCF7) procured from NCCS, Pune, India. The cells were maintained in Dulbecco's Modified Eagle Media (DMEM) with low glucose (Cat. No. -11965-092, Gibco, Invitrogen) supplemented with Antimycotic 100 X solution (Cat. No. -15240062, Thermofisher Scientific) and Fetal bovine serum (FBS) (Cat. No. -10270106, Gibco, Invitrogen). The cells were seeded in a 96-well flat-bottom microplate and maintained at  $37^\circ\text{C}$  in 95% humidity and 5%  $\text{CO}_2$  overnight [63, 64].

### Anti-tubercular activity

The anti-tubercular activity of compounds has screened against *Mycobacterium tuberculosis* (vaccine strain,  $\text{H}_{37}\text{R}_v$ , ATCC No. -27294, density— $3 \times 10^5$  CFU/ml, state—liquid suspension). Microplate Alamar Blue assay (MABA) method have used to test the anti-tubercular activities [65, 66]. 200  $\mu\text{l}$  of sterile deionized water was added to all outer perimeter wells of sterile 96 wells plate to minimized evaporation of medium in the test wells during incubation. The 96 wells plate received 100  $\mu\text{l}$  of the Middlebrook 7H9 broth and serial dilution of compounds were made directly on plate. The final drug concentrations tested were 100–0.8  $\mu\text{g}/\text{ml}$ . Plates were covered and sealed with parafilm and incubated at  $37^\circ\text{C}$  for five days. After this time, 25  $\mu\text{l}$  of freshly prepared 1:1 mixture of Almar Blue reagent and 10% tween 80 was added to the plate and incubated for 24 h. A blue color in the well was interpreted as no bacterial growth, and pink color was scored as growth. The MIC was defined as lowest drug concentration which prevented the color change from blue to pink.

## Computational methods

### Ligand library preparation

The chemical structures synthesized tetrahydropyridines (**4a–4h**) were designed and drawn using ACD/ChemSketch software [67]. Using BIOVIA Discovery Studio, hydrogen atoms were added to the designed structures [68]. The energy minimization (EM) of protonated ligands were performed using the MMFF94 force field with steepest descent algorithm. The resulting optimized ligand structures were then converted into pdbqt files compatible with AutoDock vina, utilizing the OpenBabel plugin of PyRx 0.8 [69, 70]. A prepared ligand library containing designed compounds were used for further in silico study.

### Theoretical drug-likeness and ADME(T) prediction

The drug-likeness and theoretical pharmacokinetic properties of the synthesized tetrahydropyridines (**4a–4h**) was assessed via the SwissADME and pkCSM servers [71, 72].

### Density functional theory (DFT) study

DFT method was used to determine frontier molecular orbitals (FMO) along with chemical, and global reactivity descriptors of synthesized tetrahydropyridines (**4a–4h**). Previously described methodologies and other experimental particulars were followed to conducting the DFT calculations [73–75]. ORCA 4.2.1 program was utilized with employing B3LYP functional and def2-SVP basis set [76]. Input file preparation and output file interpretation were facilitated using Orca-enhanced Avogadro software [77]. Chemical reactivity descriptors were calculated following the equations of Koopmans' theory [78–80].

## Molecular docking study

### Protein preparation

Previously reported 3D crystal structures of CDK2 (PDB 6GUE) having 1.99 Å resolution and *M. tuberculosis* DprE1 (PDB 4FDO) having 2.29 Å resolution was selected from literature and retrieved from the RCSB Protein data bank [81]. The retrieved protein structure was then subjected for preparation and structures was cleaned by removing water molecules and hetero atoms [82]. The ionization and tautomeric states of amino acids from cleaned protein structure corrected by protonating with polar hydrogen atoms. Protein preparation protocol was executed using BIOVIA Discovery Studio software.

## Docking

Docking study was done by utilizing the AutoDock Vina module of PyRx 0.8 [83, 84]. Initially, the prepared protein structure (PDB: 4FDO and PDB: 6GUE) was imported and subjected to EM with converting as AutoDock macromolecule. The energy-minimized protein and ligand structures were selected in AutoDock vina module and docking study was performed [85]. A maximized grid box was selected in the Vina workspace to cover the entire protein structures and exhaustiveness was set at eight [86, 87]. In order to identify the optimal conformation of docked ligands, the pose with the highest negative binding affinity was chosen and saved for further analysis. Subsequently, binding interactions of this saved pose were visualized through the BIOVIA Discovery Studio [88].

## Results and discussion

### Chemistry

The tetrahydropyridine derivatives (**4a–4h**) were obtained by one-pot multicomponent reaction of one mole of ethyl acetoacetate, two moles of substituted aromatic amines, and two moles of substituted benzaldehydes in presence of Bronsted acidic ionic liquid [MSbIM][Cl] as catalyst. Initially, we performed a reaction without catalyst with two moles of 4-methoxy aniline with one mole of ethyl acetoacetate and two moles of 4-methyl benzaldehyde in ethanol as solvent at room temperature. It was found that no desired product formation even after 24 h of time (Table 1, entry

**Table 1** Optimization of reaction conditions by using different amounts of catalyst<sup>a</sup>

Entry	Catalyst (mol%)	Temperature (°C)	Time (hr)	Yield(%) <sup>b</sup>
1	–	rt	24	NR <sup>c</sup>
2	5	rt	24	67
3	10	rt	24	76
4	15	rt	24	78
5	30	rt	12	71
6	5	70	5	83
7	5	80	5	91
8	5	100	5	91
9	10	80	3.5	93
10	15	80	3.5	96
11	30	80	3.5	96

<sup>a</sup>Reaction conditions: ethyl acetoacetate (1 mmol), 4-methoxyaniline (2 mmol), 4-methylbenzaldehyde (2 mmol), IL (15 mol%), 3 mL ethanol, reflux at 80 °C

<sup>b</sup>Isolated yields

<sup>c</sup>No reaction

**Table 2** Effect of solvent on the reaction<sup>a</sup>

Entry	Solvent	Time (hr)	Yield (%) <sup>b</sup>
1	Ethanol	3.5	96
2	Methanol	3.5	92
3	Acetonitrile	3.5	67
4	DMF	3.5	65
5	CH <sub>2</sub> Cl <sub>2</sub>	3.5	60
6	THF	3.5	72
7	Water	3.5	32, 41 <sup>c</sup>

<sup>a</sup>Reaction conditions: ethyl acetoacetate (1 mmol), 4-methoxyaniline (2 mmol), 4-methylbenzaldehyde (2 mmol), IL (15 mol%), reflux at 80 °C

<sup>b</sup>Isolated yields

<sup>c</sup>Reaction carried out at 110 °C

1). But, when the same reaction was performed in the presence of IL catalyst, we get the product with 67% yield (Table 1, entry 2). With this promising result, we next investigated the effect of amount of catalyst at different temperatures (Table 1, entries 3–11) in presence of ethanol as solvent. The best results were obtained when the reaction carried out at 80 °C temperature using 15 mol% of IL catalyst (Table 1, entry 10).

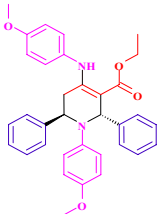
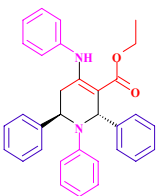
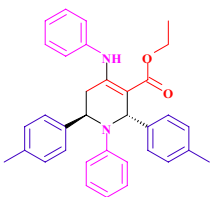
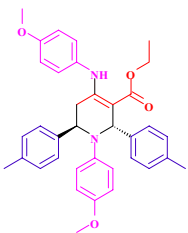
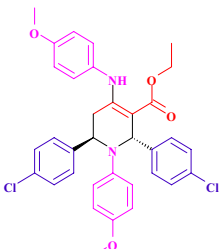
The solvent plays a very important role in transforming reactants into the products. So, we investigated effect of solvent on the reaction using different solvents such as ethanol, methanol, acetonitrile, DMF, CH<sub>2</sub>Cl<sub>2</sub>, THF and water (Table 2, entries 1–5). The excellent result was obtained in ethanol solvent than other. When we used the water as solvent, the yield was very poor due to insolubility of the reactants.

After optimization study, the standard conditions were applied with different substituted aromatic amines and substituted benzaldehydes to furnish in to tetrahydropyridines derivatives (Table 3). The highest yield has been obtained for aromatic amine carrying electron donating group like 4-methoxy aniline, 4-methyl aniline and reactive benzaldehydes such as halo substituted benzaldehydes. This is because, electron donating group stabilize the imine intermediate formed by the reaction of ethyl acetoacetate and amine in the transition state. Both the electron donating and withdrawing groups on benzaldehyde tolerated the reaction and produced expected compounds.

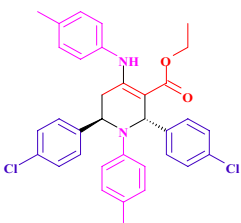
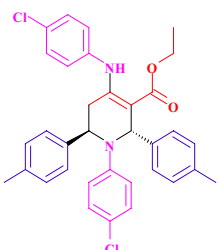
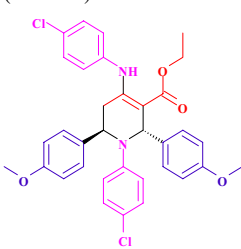
All the synthesized compounds were confirmed by spectral analysis such as IR, <sup>1</sup>H NMR and <sup>13</sup>C NMR. In the IR spectrum of compound **4d**, a band at 3246.46 cm<sup>-1</sup> represents presence of NH (bonded) group. Then bands appeared at 1652.44 and 1597.36 cm<sup>-1</sup> confirms the presence of α, β-unsaturated carbonyl group. In the <sup>1</sup>H NMR spectra of compound **4d**, triplet (*J* = 7.2 Hz) at δ 1.44 ppm is due to -CH<sub>3</sub> group of -OCH<sub>2</sub>CH<sub>3</sub>. The two singlets at δ 2.32 and δ 2.35 ppm represents two methyl groups on aldehyde benzene rings. Further, the dd signal at δ 2.61–2.66 ppm and multiplet at 4.27–4.45 ppm confirms the presence of four diastereotopic protons present at position C-6 and ethyl group of ethyl



**Table 3** Physical properties of synthesized compounds (**4a–4h**)<sup>a</sup>

Compound	Product	M. P. (Lit.) (°C)	Time (hr)	Yield (%) <sup>b</sup>
4a	 (PRK111)	170–172 (172–174) [89]	3.5	93
4b	 (PRK111/1)	169–171 (170–171) [90]	4.5	90
4c	 (PRK111/2)	229–230 (230–231) [89]	5.5	91
4d	 (PRK112)	219–221 (217–219) [89]	3.5	96
4e	 (PRK113)	187–189 (186–188) [89]	4.5	94

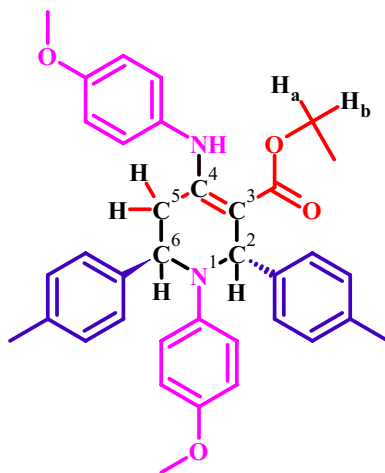
**Table 3** (continued)

Compound	Product	M. P. (Lit.) (°C)	Time (hr)	Yield (%) <sup>b</sup>
4f		242–244 (240–241) [89]	4.5	93
4g	(PRK117) 	218–219 (219–220) [91]	6.0	90
4h	(PRK121)  (PRK122)	181–183 (180–182) [91]	6.0	91

<sup>a</sup>Reaction conditions: ethyl acetoacetate (1 mmol), aniline derivative (2 mmol), benzaldehyde derivative (2 mmol), IL (15 mol%), 3 mL ethanol, reflux at 80 °C

<sup>b</sup>Isolated yields

acetoacetate. The doublet at  $\delta$  5.02 ppm ( $J=2.8$  Hz) represent single proton at C-5, and singlet at  $\delta$  6.29 ppm represents single de-shielded proton at C-2. A multiplet appears between  $\delta$  6.21 and  $\delta$  7.26 ppm is corresponding to aromatic protons. A broad singlet at  $\delta$  10.14 represents the highly de-shielded NH protons due to H-bonding via cyclic six membered ring with carbonyl oxygen of ester group. The appearance of peaks in  $^{13}\text{C}$  NMR of **4d** compound at  $\delta$  14.7, 33.5, 55.0, 58.2, 59.6, 98.2, 112.9, 116.1, 125.6, 125.7, 123.2, 126.3, 127.0, 128.1, 128.3, 128.5, 128.7, 137.8, 142.7, 144.0, 146.9, 156.0, 168.2 ppm supports the formation of compound (Fig. 1). All the other prepared derivatives have shown characteristic peaks in IR,  $^1\text{H}$  and  $^{13}\text{C}$  spectra which are in good agreement with the proposed structures and also with the literature data. (The analytical data have been provided in supplementary file).

**Fig. 1** Detailed structure parameters of compound **4d****Table 4** Comparison of the various methods used for the synthesis of tetrahydropyridine derivatives (**4a–4h**)

Entry	Catalyst (mol%)	Reaction condition	Time in hrs	Yield (%)	Reference
1	L-proline nitrate (10)	Methanol, RT	8–14	63–90	[92]
2	BF <sub>3</sub> ·SiO <sub>2</sub> (15)	Methanol, 65 °C	5–9	31–92	[93]
3	TBBDA	Ethanol, RT	7–20	68–90	[94]
4	[Hpyro][HSO <sub>4</sub> ] (15)	Ethanol, reflux	8–14	33–82	[95]
5	EDDF (25)	Ethanol, reflux	5.5–10	47–90	[96]
6	5-SSA (20)	Methanol, RT	4–12	28–93	[97]
7	[MSbIM-Cl] (15)	Ethanol, 80 °C	3.5–6	90–96	<b>This work</b>

RT room temperature

To check the efficacy of our IL catalyst, we compared the present reaction conditions with earlier reported methods for the synthesis of tetrahydropyridine derivatives (Table 4). This comparison study reveals that our catalyst has some advantages over the other reported methods such as less reaction time with high yields of the products.

## Biological activities

### In-vitro anticancer activity

The synthesized derivatives of tetrahydropyridine were screened against human breast cancer cell line (MCF-7) by using 3-(4,5-dimethylthiazol-2-yl)-2,5-diphenyl tetrazolium bromide (MTT) assay (Table 5). The cultured cells were treated with different concentrations (100, 50, 25, 12.5, 6.25, and 3.125 µg/ml) of samples and incubated for 48 h. The wells were washed twice with PBS and 20 µL of the MTT staining solution was added to each well and the plate was incubated at 37 °C. After 4 h, 100 µL of DMSO

**Table 5** Cell viability at 100 µg/ml and IC<sub>50</sub> values for synthesized tetrahydropyridine derivatives (**4a–4h**)

Compound	Cell viability (100 µg/ml)	IC <sub>50</sub> (µg/ml)
4a	17.76	45.08
4b	20.34	44.65
4c	21.49	48.34
4d	19.23	46.48
4e	11.77	34.19
4f	18.31	40.71
4g	23.7	52.65
4h	17.85	47.71
Standard*	11.56	1.77

\*Doxorubicin, negative control = 100 µg/ml

was added to each well to dissolve the formazan crystals, and absorbance was recorded with a 570 nm using microplate reader. Then, the cytotoxicity of samples was determined by using following relation,

$$\text{Surviving cells(\%)} = \text{Mean OD of test compound} / \text{Mean OD of Negative control} \times 100$$

Cell viability data of all the synthesized compound (**4a–4h**) showed potent anti-cancer activities against the MCF7 cell line at the concentration of 100 µg/ml in comparison with the standard drug Doxorubicin (Fig. 2). The activity decreases as the concentration of synthesized compounds decreases. The compound **4e** showed the highest activity amongst other tetrahydropyridine derivatives (Fig. 3).

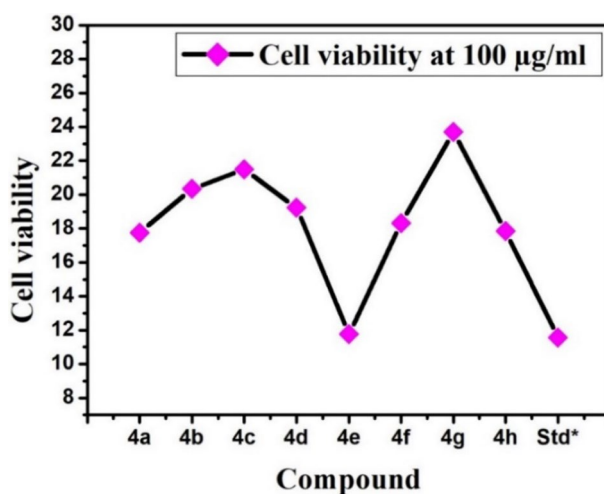


**Fig. 2** Cell viability of synthesized compounds at 100 µg/ml, Std\* = Doxorubicin

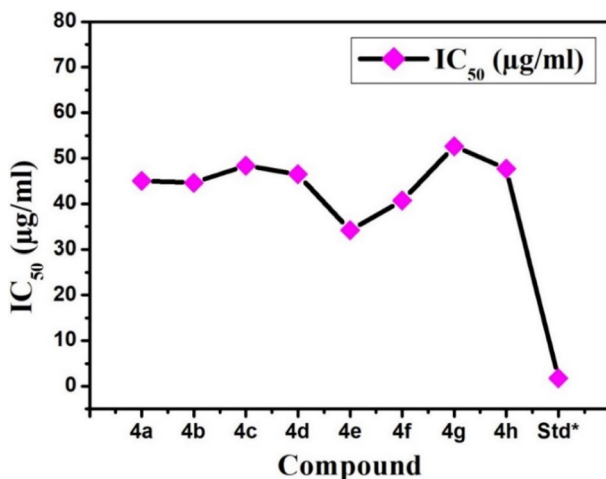


**Fig. 3** IC<sub>50</sub> values of synthesized compounds, Std\* = Doxorubicin

### In-vitro anti-tubercular activity

The antitubercular activities of all the synthesized compounds were assessed against *Mycobacterium tuberculosis* using microplate alamar blue assay (MABA). This methodology is nontoxic, uses thermally stable reagent, and shows good correlation with proportional and BACTEC radiometric method. The compounds **4a–4h** series

**Table 6** Anti-tubercular activities against *Mycobacterium tuberculosis*

Compound	100 µg/ml	50 µg/ml	25 µg/ml	12.5 µg/ml	6.25 µg/ml	3.12 µg/ml	1.6 µg/ml	0.8 µg/ml
4a	S	R	R	R	R	R	R	R
4b	S	S	S	R	R	R	R	R
4c	S	R	R	R	R	R	R	R
4d	S	S	S	R	R	R	R	R
4e	S	S	R	R	R	R	R	R
4f	S	S	R	R	R	R	R	R
4g	S	S	R	R	R	R	R	R
4h	S	S	S	S	R	R	R	R
isoniazid	S	S	S	S	S	S	S	R
ethambutol	S	S	S	S	S	S	S	R
pyrazinamide	S	S	S	S	S	S	R	R
rifampicin	S	S	S	S	S	S	S	S
streptomycin	S	S	S	S	S	S	S	S

S sensitive, R resistant

were screened for antimycobacterial activity against *Mycobacterium tuberculosis* (ATCC-27294) at concentrations of **100–0.8 µg/ml** by using standard drugs such as isoniazid, ethambutol, pyrazinamide, rifampicin, streptomycin (Table 6).

The results confirmed that all compounds (**4a–4h**) illustrate activity at concentrations of **50** and **100 µg/ml** except compound **4a** and **4c**. The compounds **4b**, **4d** and **4h** showed effective activity at concentration of **25 µg/ml**. The only compound **4h** showed the effective activity at concentration of **12.5 µg/ml**. All the compounds were found to be inactive at concentration of **6.25–0.8 µg/ml**.

## Computational methods

### Theoretical drug-likeness and ADME(T) prediction

In current study, drug-likeness assessment of synthesized tetrahydropyridine derivatives (**4a–4h**) was conducted by evaluating their physicochemical properties and applying Lipinski's rule of five (Ro5) and Veber's rule. The calculated physicochemical properties and drug-likeness prediction was represented in Table 7. Lipinski's Ro5 based on empirical data, suggests that compounds with a molecular weight <500 Daltons, logP values less than 5, fewer than 5 hydrogen bond donors, and total polar surface area (TPSA) under 140 Å are more likely to be orally bioavailable and promising drug candidates [98–100]. On the other hand Veber's rule focuses on compound flexibility and restricts the number of rotatable bonds to 10 [101]. All compounds explored in the study met criteria of Veber's rule. The fewer rotatable bonds in these compounds align with the concept that compounds with limited flexibility tend to exhibit improved pharmacokinetics and potential as drug candidates. However, the Lipinski's Ro5 resulted in negative outcomes for the majority of the synthesized tetrahydropyridine derivatives, with the exception of compound **4h**. Although the compounds failed to satisfy Lipinski's Ro5, various recent research has demonstrated that several modern drugs not adhering to traditional Ro5 guidelines can still exhibit favorable pharmacokinetics and therapeutic properties.

**Table 7** Drug-likeness property prediction of synthesized tetrahydropyridine derivatives (**4a–4h**)

Compound	MW (g/mol)	mLogP	HBA	HBD	MR	TPSA	nRot	Lipinski's rule (Ro5)	Veber's rule
4a	562.7	4.56	4	1	171.84	60.03	10	–	+
4b	502.65	5.31	2	1	158.86	41.57	8	–	+
4c	603.53	5.1	4	1	171.93	60.03	10	–	+
4d	534.64	4.2	4	1	161.91	60.03	10	–	+
4e	571.54	6.2	2	1	168.88	41.57	8	–	+
4f	571.54	6.2	2	1	168.88	41.57	8	–	+
4g	603.53	5.1	4	1	171.93	60.03	10	–	+
4h	474.59	4.94	2	1	148.92	41.57	8	+	+

MW molecular weight; mLogP lipophilicity; HBA hydrogen bond acceptor, HBD hydrogen bond donor, MR molar refractivity, TPSA topological polar surface area, nRot number of rotatable bonds

**Table 8** In silico ADMET property prediction of synthesized tetrahydropyridine derivatives (**4a–4h**)

Entry	Absorption		Distribution		Metabolism		Excretion		Toxicity	
	Intestinal absorption (human)	VDss (human)	BBB permeability	CNS permeability	Substrate	Inhibitor	Total clearance	AMES toxicity	Numeric (log mL min <sup>-1</sup> kg <sup>-1</sup> )	Categorical (yes/no)
	Numeric (%absorbed)	Numeric (log L kg <sup>-1</sup> )	Numeric (log BB)	Numeric (log PS)	CYP					
					2D6	3A4 1A2 2C19 2C9 2D6 3A4				
<b>4a</b>	94.45	-0.32	-0.54	-1.68	No	Yes No Yes No Yes No	Yes	Yes	0.42	No
<b>4b</b>	93.91	-0.33	0.20	-0.06	No	Yes No Yes No Yes No	Yes	Yes	0.54	Yes
<b>4c</b>	93.58	-0.19	0.24	-0.05	No	Yes No Yes No Yes No	Yes	Yes	0.55	Yes
<b>4d</b>	94.17	-0.19	-0.51	-1.51	No	Yes No Yes No Yes No	No	Yes	0.43	No
<b>4e</b>	91.25	-0.18	-0.53	-1.43	No	Yes No Yes No Yes No	No	Yes	-0.04	No
<b>4f</b>	89.72	-0.03	0.26	0.03	No	Yes No Yes No Yes No	No	Yes	-0.21	No
<b>4g</b>	89.72	-0.03	0.26	0.03	No	Yes No Yes No Yes No	No	Yes	-0.21	No
<b>4h</b>	91.28	-0.21	-0.51	-1.40	No	Yes No Yes No Yes No	No	Yes	-0.04	No

The performed *in silico* ADMET study on the synthesized tetrahydropyridine derivatives (**4a–4h**) provided valuable insights into their pharmacokinetic and safety attributes. pkCSM was utilized for the prediction of pharmacokinetic (ADMET) properties [72]. Predicted properties are pivotal for determining their potential as drug candidates. Predicted ADMET values are detailed in Table 8. Assessment of human intestinal absorption indicated favorable results, with absorption rates exceeding 90% for most synthesized derivatives, except for compounds **4f** and **4g**. This prediction of human intestinal absorption suggests that these compounds may exhibit robust oral bioavailability. The evaluation of volume of distribution (VD<sub>ss</sub>) indicated acceptable values with logVD<sub>ss</sub> exceeding  $-0.15$  for all compounds, except compounds **4f** and **4g**. These findings of VD<sub>ss</sub> indicates reasonable distribution of these compounds within the body. In the case of assessment of blood–brain barrier (BBB) permeability, it is worth noting that a logBB greater than 0.3 suggests that a compound may easily cross the BBB. While a logBB lower than  $-1$  indicates limited distribution of compounds to the brain. In this case, the predicted logBB values of synthesized compounds suggested restricted brain distribution as they exhibited logBB values below  $-1$ . Additionally, central nervous system (CNS) permeability (logPS) predictions suggested that synthesized compounds do not possess the ability to permeate the CNS. Metabolism profiling of the synthesized compounds was found to be satisfactory with all the compounds showing CYP3A4 substrate characteristics. Excretion profile of synthesized compounds fell within acceptable ranges supporting their candidacy as drug candidates. Importantly, all the compounds, except for **4b** and **4c**, exhibited a favorable *in silico* toxicity profile suggesting an absence of AMES toxicity and mutagenic properties. These findings provide confidence in the safety aspects of the synthesized tetrahydropyridine derivatives (**4a–4h**). The results of the *in silico* ADMET and drug-likeness assessments offered a basis for the understanding of the pharmacokinetic characteristics, safety profiles, and potential for optimization of tetrahydropyridine derivatives (**4a–4h**). While certain variations and inhibitory properties were observed. Results of this study encourage further investigations and refinement of these compounds.

### DFT study

The tetrahydropyridine derivatives (**4a–4h**) underwent a DFT investigation to determine their frontier molecular orbitals (FMOs) and establish a correlation with the binding interactions identified in the docking study. According to the FMO theory, the bioactivity of small molecules exhibits an association with the energy levels of their highest occupied molecular orbital (HOMO) and lowest unoccupied molecular orbital (LUMO) [102, 103]. FMO theory further suggests that chemical reactions require electron interactions between the HOMO of one compound and the LUMO of another compound. HOMOs serve as sources for electron donation, on the other hand LUMOs act as electron acceptors in these reaction processes [104]. This electron transfer mechanism is a fundamental aspect of understanding chemical reactivity. FMO exerts pivotal role in pharmacological characterization and contribute valuable insights into the mechanisms of biochemical interactions. The computation of quantum chemical parameters was undertaken to elucidate the reactivity and



stability of the synthesized tetrahydropyridine derivatives [105]. These parameters encompass properties such as molecular orbital energies and global chemical reactivity descriptors. Additionally, understanding these quantum properties aids in predicting how these compounds may interact with specific biological targets.

In accordance with findings from study of Rochlani et al., a compound displaying an elevated value for the HOMO–LUMO energy gap (HLG) manifests a less reactive disposition [73, 106]. On the other hand, a narrower HLG signifies high reactivity which may be related with a greater likelihood of enhanced biological activity for the compound. This insight brings into line with the principle that a smaller HLG facilitates electron transfer processes, which are important to chemical reactivity and biological interactions. The HLG served as a crucial determinant in assessing the reactivity and bioactivity potential of chemical compounds [73, 106, 107]. The synthesized tetrahydropyridine derivatives (**4a–4h**) can be ranked in terms of their chemical reactivity based on the HLG, as follows: **4a** > **4e** > **4d** > **4g** > **4c** > **4h** > **4b** > **4f**. Figure 4 illustrates the FMOs of these synthesized derivatives. Table 9 provides the calculated global chemical reactivity descriptors and HOMO and LUMO energy values for these compounds. The distribution of charge within a compound is crucial for assessing both intramolecular and intermolecular interactions [108]. The dipole moment (DM) serves as a key electronic parameter directly linked to the charge distribution in a compound [109]. It is utilized to estimate the intensity of intermolecular interactions resulting from the non-uniform distribution of charges among the atoms in the investigated compounds. Therefore, the DM values calculated via

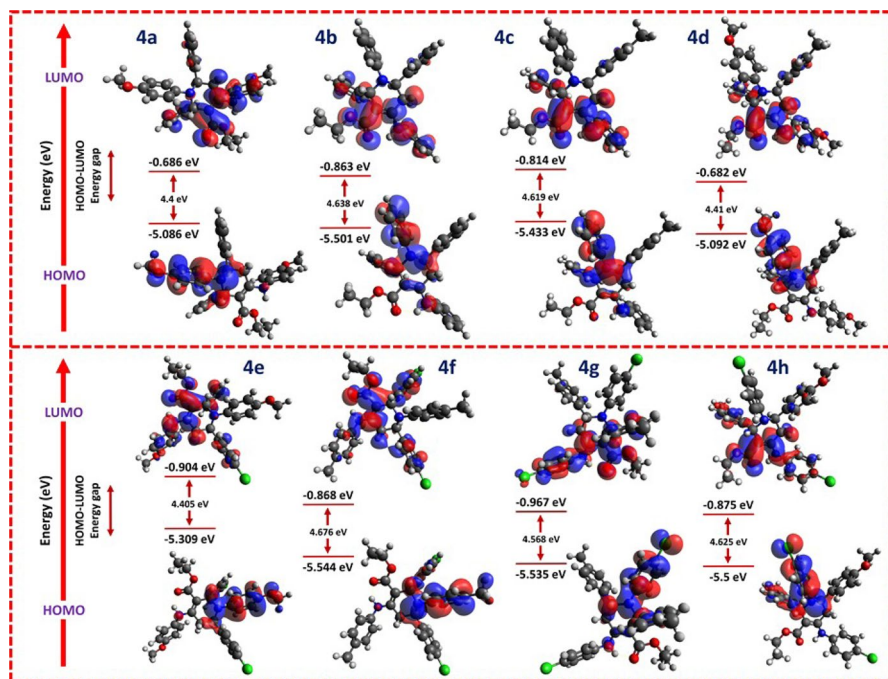


Fig. 4 HOMO–LUMO and energy gap (HLG) of tetrahydropyridine derivatives (**4a–4h**)

**Table 9** Calculated FMO and global chemical reactivity descriptors for tetrahydropyridine derivatives (**4a–4h**)

Entry	HOMO (eV)	LUMO (eV)	HLG (eV)	DM (Debye)	IP (eV)	EA (eV)	$\chi$ (eV)	$\mu$ (eV)	$\eta$ (eV)	$\omega$ (eV)
4a	-5.09	-0.69	4.40	2.01	5.09	0.69	2.89	-2.89	2.20	1.89
4b	-5.50	-0.86	4.64	0.66	5.50	0.86	3.18	-3.18	2.32	2.18
4c	-5.43	-0.81	4.62	1.07	5.43	0.81	3.12	-3.12	2.31	2.11
4d	-5.09	-0.68	4.41	4.34	5.09	0.68	2.89	-2.89	2.21	1.89
4e	-5.31	-0.90	4.41	1.45	5.31	0.90	3.11	-3.11	2.20	2.19
4f	-5.54	-0.87	4.68	0.74	5.54	0.87	3.21	-3.21	2.34	2.20
4g	-5.54	-0.97	4.57	2.84	5.54	0.97	3.25	-3.25	2.28	2.31
4h	-5.50	-0.88	4.63	7.94	5.50	0.88	3.19	-3.19	2.31	2.20

HOMO: highest occupied molecular orbital; LUMO: lowest unoccupied molecular orbital; HLG: HOMO–LUMO gap; DM: dipole moment; IP: ionization potential; EA: electron affinity;  $\chi$ : electronegativity;  $\mu$ : chemical potential;  $\eta$ : chemical hardness;  $\omega$ : electrophilicity

theoretical methods hold significant importance. A high DM indicates a greater degree of molecular polarity [108, 110]. The order of compounds, ranked from high to low DM is as follows: **4h** > **4d** > **4g** > **4a** > **4e** > **4c** > **4f** > **4b**. Compound **4h** exhibited the highest DM at 7.94 Debye, while compound **4b** displayed the lowest.

Koopman's theorem utilizes the ionization potential (IP) and electron affinity (EA) of examined compounds to describe the ability of the HOMO and LUMO to donate and accept electrons, respectively [103, 107, 111]. IP and EA associated with synthesized tetrahydropyridine derivatives (**4a–4h**) can be calculated as the negative of their energy of HOMO and LUMO values, respectively. The IP values represented the energy needed to remove an electron from the valence band (HOMO) [112]. Previously reported literatures suggests that compounds with higher IP values exhibits greater chemical stability and inertness [113–115]. IP essentially refers to the minimum energy required to remove an electron from a compound, linked with energy of HOMO [116]. On the other hand, EA refers to the energy released by adding an electron to an atom or compound, associated with LUMO [116]. The IP of these synthesized compounds can be ordered as **4f** > **4g** > **4b** > **4h** > **4c** > **4e** > **4d** > **4a**. Notably, compound **4f** registers the highest IP, indicating a strong possibility for electron removal during chemical reactions, with a value of 5.54 eV. In terms of EA, the hierarchy from high to low is **4g** > **4e** > **4h** > **4f** > **4b** > **4c** > **4a** > **4d**. Compound **4g** demonstrates the highest EA, with a value of 0.97 eV. These diverse quantum chemical parameters provided valuable insights into the reactivity and potential utility of the synthesized tetrahydropyridine derivatives (**4a–4h**). Understanding IP and EA values of synthesized tetrahydropyridine derivatives helped to determine electronegativity ( $\chi$ ) and reflected the ability of an atom or group of atoms to attract electrons towards itself.  $\chi$  characterizes an ability of compounds to attract incoming electrons [116]. It is associated with the chemical potential ( $\mu$ ) having negative values and it signifies stability of compounds. Similarly, chemical hardness ( $\eta$ ) offers insights into their reactivity [111, 113]. The highest obtained  $\eta$  value is 2.34 eV in **4f**, diminishing to 2.32 eV in **4b**. The lowest hardness value, 2.20 eV, is observed in **4a** and **4e**. The descending order of  $\eta$  is **4f** > **4b** > **4h** > **4c** > **4g** > **4d** > **4a** > **4e**. This order correlates well with HLG, indicating that compounds with higher HLG values are characterized as hard compounds with superior kinetic stability and reduced reactivity. Such compounds resilience against electronic configuration changes.

The comprehensive outcomes of executed DFT calculations indicated that all the synthesized tetrahydropyridine derivatives possess a notably good reactivity towards chemical reactions. In the current investigation, HLG emerged as a pivotal gauge of determining molecular reactivity and kinetic stability. The observed HLG signified a high degree of chemical reactivity essentially denoting the close proximity of these energy levels. This proximate positioning suggests a minimal energy input required for facilitating electron transitions between the HOMO and LUMO orbitals, thereby promoting facile electron transfer during chemical reactions [117, 118]. However, it is crucial to acknowledge that the reduced HOMO–LUMO gap is an indicative of high chemical reactivity and may inherently have a reduced kinetic stability [119–121]. This is reflected in the ranking of synthesized compounds according to their kinetic stability, which follows a

decreasing order of  $4a < 4e < 4d < 4g < 4c < 4h < 4b < 4f$ . This observation underscores the utility of the HOMO–LUMO gap as a predictive metric for evaluating the reactivity patterns and kinetic stability of the synthesized tetrahydropyridine derivatives (**4a–4h**). Consequently, this DFT study contributes valuable insights into the stability and reactivity profiles of the above-mentioned tetrahydropyridine derivatives (**4a–4h**).

### Molecular docking study

The current investigation involved a docking study of synthesized tetrahydropyridine derivatives (**4a–4h**) to evaluate binding interactions and affinity of respective compounds towards two distinct molecular targets of cancer and tuberculosis, CDK2 (PDB 6GUE) and DprE1 (PDB 4FDO). This approach mainly focused to elucidate the potential anticancer and antitubercular properties of these compounds (**4a–4h**). The resulting binding affinity and interactions of the docked compounds with CDK2 (PDB 6GUE) and DprE1 (PDB 4FDO) obtained via docking study are summarized in Table 9. Regarding the anticancer potential against CDK2 (PDB 6GUE),

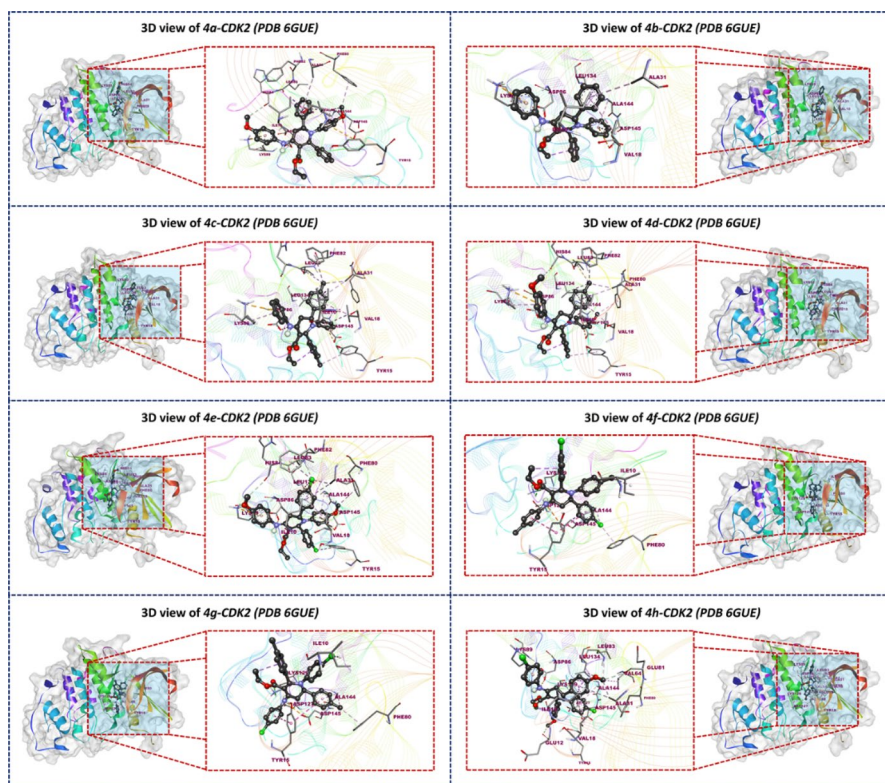


**Fig. 5** Binding interaction of the synthesized tetrahydropyridine derivatives (**4a–4h**) with CDK2 (PDB 6GUE)

all synthesized compounds (**4a–4h**) exhibited binding affinities within the range of  $-9.5$  to  $-10.2$  kcal/mol. The 3D binding orientations of these compounds with CDK2 (PDB 6GUE) are visually represented in Fig. 5.

Compound **4d** demonstrated the most favorable binding affinity with CDK2 (PDB 6GUE) among the tested tetrahydropyridine derivatives with a binding affinity of  $-10.2$  kcal/mol. Notably, compound **4d** engaged in several critical interactions with the target protein. These interactions included a  $\pi$ -cation interaction with Asp145, a carbon-hydrogen bond with His84, a  $\pi$ -anion interaction with Lys89, an attractive charge interaction with Asp86, and  $\pi$ -sigma type interactions with Ile10 and Leu134. Additionally, it exhibited hydrophobic interactions in the form of alkyl and  $\pi$ -alkyl interactions with Val18, Ala31, Ala144, Leu83, Phe82, Phe80, Tyr15, and Leu134.

Compound **4c** and **4e** also displayed significant binding affinities of  $-10.1$  kcal/mol and  $-10$  kcal/mol, respectively. The binding interactions of compound **4c** included a  $\pi$ -cation interaction with Asp145, a  $\pi$ -anion interaction with Lys89, an attractive charged interaction with Asp86, and  $\pi$ -sigma bonding with Ile10 and Leu134. Furthermore, hydrophobic interactions were observed with Val18, Ala31, Ala144, Leu83, Phe82, Leu134, and Tyr15. In the context of anticancer potential, compound **4e** exhibited remarkable cell viability and an  $IC_{50}$  value in in vitro screening suggesting possibility of promising anticancer activity. This compound, akin to **4d** and **4c**, formed strong binding interactions with CDK2. The results underscore the potential of these tetrahydropyridine derivatives as candidates for further optimization and exploration in anticancer agent development.

In the evaluation of the anti-tubercular potential of the synthesized compounds against DprE1 (PDB 4FDO), a range of binding affinities, spanning from  $-6.9$  to  $-9.9$  kcal/mol, was observed. The binding orientation of docked compounds against DprE1 (PDB 4FDO) represented in Fig. 6. Compound **4b** exerted highest negative binding affinity of  $-9.9$  kcal/mol and formed conventional hydrogen bond with Tyr60, carbon-hydrogen bond with Gly321,  $\Pi$ -sulfur interaction formed with Cys387, His132 showed  $\Pi$ -cation, Val365, Thr118, and Trp16 involved in formation of  $\Pi$ -sigma, Arg58 and Leu363 involved in formation  $\Pi$ -alkyl with compound **4b**.

In an extension to the investigation, compound **4g** demonstrated the second-highest negative binding affinity, amounting to  $-8.7$  kcal/mol, when interacting with the targeted DprE1 (PDB 4FDO). Notably, compound **4g** forged notable interactions with specific amino acid residues, including Asp232, Phe362, Phe320, His315, Met319, Pro316, Ala244, and Ile234, involving diverse interaction types such as  $\pi$ -anion,  $\pi$ - $\pi$  stacked, alkyl, and  $\pi$ -alkyl interactions, as outlined in Table 10. These findings illuminate the multifaceted binding interactions of compound **4g** with the DprE1 protein, indicating a strong and versatile binding profile. The presence of  $\pi$ -anion and  $\pi$ - $\pi$  stacked interactions underscores the compound's ability to form crucial non-covalent bonds with the targeted protein. However, formation of alkyl and  $\pi$ -alkyl interactions could contribute to the stability of the compound within the binding site. The outcomes of the docking study unveiled promising results for all the docked compounds when interacting with the structures of the targeted proteins, CDK2 (PDB 6GUE) and DprE1 (PDB 4FDO).



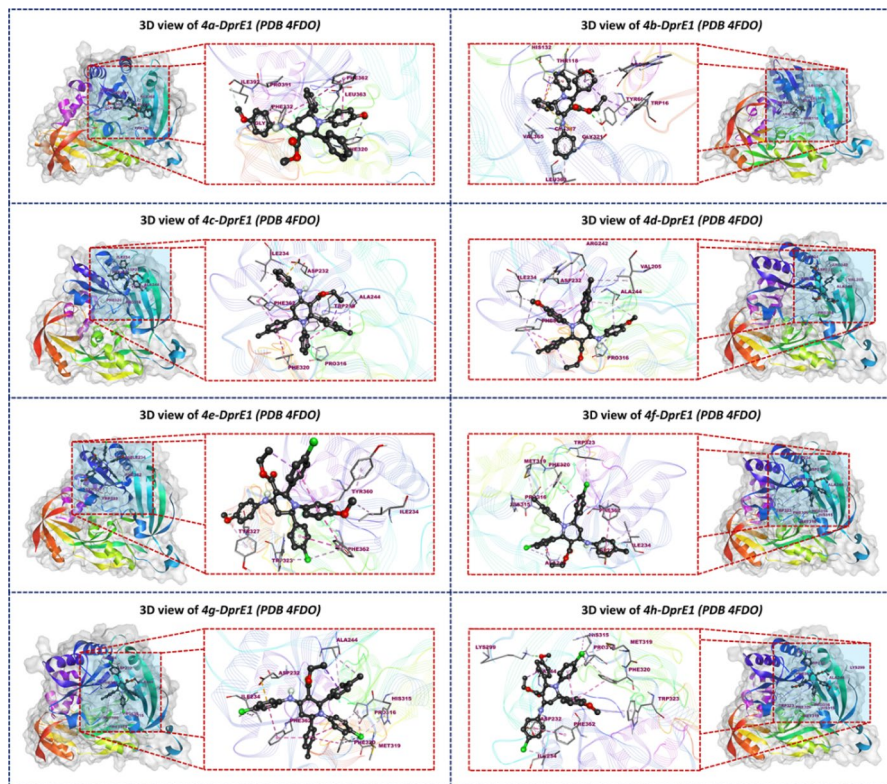


**Fig. 6** Binding interaction of the synthesized tetrahydropyridine derivatives (**4a–4h**) with DprE1 (PDB 4FDO)

## Conclusion

In summary, we achieved an easy and efficient synthesis of highly functionalized tetrahydropyridine derivatives using Bronsted acidic ionic liquid. The compounds were obtained in excellent yields without the aid of chromatographic purification. Metal-free synthesis, easy workup, no harsh reaction conditions, less reaction time, easily available starting materials are remarkable features in comparison with traditional methods. The compound **4e** displayed the highest anticancer activity against MCF7 cell lines while the compound **4h** displayed the highest anti-tubercular activity against mycobacterium tuberculosis. The docking study revealed that all the synthesized derivatives have shown good interactions against **CDK2** and **DprE1** with the binding energy ranges between  $-10.2$  to  $-9.5$  kcal/mol and  $-9.9$  to  $-6.9$  kcal/mol respectively. DFT study gives valuable information about the stability and reactivity of synthesized derivatives. Other studies such as in silico ADMET prediction and drug-likeness emphasize the synthesized derivatives would be modified for further pharmacological studies thereby in search of potential lead compound.

**Table 10** Binding affinity and interactions for tetrahydropyridine derivatives (**4a–4h**) docked against (PDB 6GUE) and (PDB 4FDO)

Entry	CDK2 (PDB 6GUE)				DprE1 (PDB 4FDO)			
	Binding affinity (kcal/mol)	Interactions	Type of interaction	Distance	Binding affinity (kcal/mol)	Interactions	Type of interaction	Distance
<b>4a</b>	-9.7	His84	C-H bond	3.56	-7.2	Ile392	C-H bond	3.77
		Asp145	$\Pi$ -cation	4.81		Gly331	C-H bond	3.49
		Asp86	Attractive charge	3.69		Phe362	$\Pi$ -donor H bond	3.06
		Lys89	$\Pi$ -anion	4.06		Phe332	$\Pi$ - $\Pi$ stacked	4.91
		Leu134	$\Pi$ -sigma	3.84		Phe362	$\Pi$ - $\Pi$ T shaped	4.53
		Ile10	$\Pi$ -sigma	3.76		Phe320	$\Pi$ -alkyl	4.53
		Ala144	Alkyl, $\Pi$ -alkyl	4.18, 5.20		Leu363	$\Pi$ -alkyl	3.06, 5.21
		Phe80	Alkyl, $\Pi$ -alkyl	4.22		Pro391	$\Pi$ -alkyl	5.25
		Val18	Alkyl, $\Pi$ -alkyl	5.13, 5.18				
		Ala31	Alkyl, $\Pi$ -alkyl	5.06				
	<b>4b</b>	-9.5	Asp145	$\Pi$ -cation	4.69	-9.9	Tyr60	Conventional H Bond
		Lys89	$\Pi$ -anion	4.09		Gly321	C-H bond	3.40
		Asp86	Attractive charge	3.79		Cys387	$\Pi$ -sulfur	5.91
		Ile10	$\Pi$ -sigma	3.78		His132	$\Pi$ -cation	3.86, 4.56
		Leu134	$\Pi$ -sigma	3.82		Val365	$\Pi$ -sigma	3.85
		Val18	Alkyl, $\Pi$ -alkyl	5.16, 5.19		Thr118	$\Pi$ -sigma	3.75
		Ala31	Alkyl, $\Pi$ -alkyl	5.02		Trp16	$\Pi$ -sigma	3.71
		Ala144	Alkyl, $\Pi$ -alkyl	5.26		Arg58	$\Pi$ -alkyl	4.85
						Leu363	$\Pi$ -alkyl	4.81

Table 10 (continued)

Entry	CDK2 (PDB 6GUE)			DprE1 (PDB 4FDO)				
	Binding affinity (kcal/mol)	Interactions	Type of interaction	Distance	Binding affinity (kcal/mol)	Interactions	Type of interaction	Distance
<b>4c</b>	-10.1	Asp145	$\Pi$ -cation	4.69	-8.3	Trp230	C-H bond	3.76
		Lys89	$\Pi$ -anion	4.10		Asp232	$\Pi$ -anion	3.54
		Asp86	Attractive charge	3.72		Phe362	$\Pi$ - $\Pi$ stacked	4.63, 5.03
		Ile10	$\Pi$ -sigma	3.86		Phe320	$\Pi$ - $\Pi$ stacked	5.82
		Leu134	$\Pi$ -sigma	3.75		Pro316	Alkyl, $\Pi$ -alkyl	4.95
		Val18	Alkyl, $\Pi$ -alkyl	5.18, 5.29		Ala244	Alkyl, $\Pi$ -alkyl	4.36, 4.51
		Ala31	Alkyl, $\Pi$ -alkyl	3.46, 5.08		Ile234	Alkyl, $\Pi$ -alkyl	4.88
		Ala144	Alkyl, $\Pi$ -alkyl	5.23				
		Leu83	Alkyl, $\Pi$ -alkyl	4.99				
		Phe82	Alkyl, $\Pi$ -alkyl	4.85				
		Leu134	Alkyl, $\Pi$ -alkyl	5.11				
		Tyr15	Alkyl, $\Pi$ -alkyl	5.24				



**Table 10** (continued)

Entry	CDK2 (PDB 6GUE)				DprE1 (PDB 4FDO)			
	Binding affinity (kcal/mol)	Interactions	Type of interaction	Distance	Binding affinity (kcal/mol)	Interactions	Type of interaction	Distance
<b>4d</b>	-10.2	Asp145	$\Pi$ -cation	4.77	-8.4	Asp232	C-H bond	3.46
		His84	C-H bond	3.72		Phe362	$\Pi$ -sigma	3.95
		Lys89	$\Pi$ -anion	4.05		Phe362	$\Pi$ - $\Pi$ stacked	5.15
		Asp86	Attractive charge	3.73		Ile234	Alkyl, $\Pi$ -alkyl	4.00
		Ile10	$\Pi$ -sigma	3.76		Phe362	Alkyl, $\Pi$ -alkyl	4.66
		Leu134	$\Pi$ -sigma	3.88		Arg242	Alkyl, $\Pi$ -alkyl	3.50
		Val18	Alkyl, $\Pi$ -alkyl	5.05, 5.08		Val205	Alkyl, $\Pi$ -alkyl	4.58
		Ala31	Alkyl, $\Pi$ -alkyl	3.65, 5.06		Ala244	Alkyl, $\Pi$ -alkyl	4.10, 4.21
		Ala144	Alkyl, $\Pi$ -alkyl	4.22, 5.39		Pro316	Alkyl, $\Pi$ -alkyl	5.26
		Leu83	Alkyl, $\Pi$ -alkyl	4.88				
		Phe82	Alkyl, $\Pi$ -alkyl	4.79				
		Phe80	Alkyl, $\Pi$ -alkyl	4.36				
		Tyr15	Alkyl, $\Pi$ -alkyl	5.20				
		Leu134	Alkyl, $\Pi$ -alkyl	4.98				

Table 10 (continued)

Entry	CDK2 (PDB 6GUE)			DprE1 (PDB 4FDO)				
	Binding affinity (kcal/mol)	Interactions	Type of interaction	Distance	Binding affinity (kcal/mol)	Interactions	Type of interaction	Distance
<b>4e</b>	-10	Asp145	$\Pi$ -cation	4.75	-6.9	Try327	C-H bond	3.79
		Lys89	$\Pi$ -anion	4.06		Phe362	$\Pi$ - $\Pi$ T shaped	5.19, 5.22
		Asp86	Attractive charge	3.63		Ile234	Alkyl, $\Pi$ -alkyl	4.66
		His84	C-H bond	3.62		Tyr360	Alkyl, $\Pi$ -alkyl	4.52
		Ile10	$\Pi$ -sigma	3.76		Phe362	Alkyl, $\Pi$ -alkyl	4.83
		Leu134	$\Pi$ -sigma	3.88		Trp323	Alkyl, $\Pi$ -alkyl	4.51
		Val18	Alkyl, $\Pi$ -alkyl	5.05, 5.08				
		Ala31	Alkyl, $\Pi$ -alkyl	3.51, 5.02				
		Ala144	Alkyl, $\Pi$ -alkyl	4.26, 5.31				
		Leu83	Alkyl, $\Pi$ -alkyl	4.85				
		Phe82	Alkyl, $\Pi$ -alkyl	4.72				
		Phe80	Alkyl, $\Pi$ -alkyl	4.28				
		Tyr15	Alkyl, $\Pi$ -alkyl	5.20				
		Leu134	Alkyl, $\Pi$ -alkyl	5.16				

Table 10 (continued)

Entry	CDK2 (PDB 6GUE)				DprE1 (PDB 4FDO)			
	Binding affinity (kcal/mol)	Interactions	Type of interaction	Distance	Binding affinity (kcal/mol)	Interactions	Type of interaction	Distance
<b>4f</b>	-9.6	Lys129	Conventional H Bond	5.40	-8.6	Asp232	$\Pi$ -anion	3.56
		Asp145	Attractive charge	3.69		Phe362	$\Pi$ - $\Pi$ stacked	4.57, 5.12
		Asp127	Attractive charge	5.21		Phe320	$\Pi$ - $\Pi$ stacked	5.76
		Asp145	$\Pi$ -sigma	3.80		His315	Alkyl, $\Pi$ -alkyl	4.59
		Tyr15	$\Pi$ - $\Pi$ T shaped	5.14, 5.95		Phe320	Alkyl, $\Pi$ -alkyl	4.95
		Phe80	Alkyl, $\Pi$ -alkyl	3.70		Met319	Alkyl, $\Pi$ -alkyl	4.71
		Ala144	Alkyl, $\Pi$ -alkyl	4.09, 4.34		Pro316	Alkyl, $\Pi$ -alkyl	4.62, 5.10
		Ile10	Alkyl, $\Pi$ -alkyl	3.74		Ala244	Alkyl, $\Pi$ -alkyl	4.44, 4.73
						Ile234	Alkyl, $\Pi$ -alkyl	4.08, 4.95
						Trp232	Alkyl, $\Pi$ -alkyl	5.38
<b>4g</b>	-9.6	Lys129	Conventional H Bond	5.35	-8.7	Asp232	$\Pi$ -anion	3.52
		Asp145	Attractive charge	3.62		Phe362	$\Pi$ - $\Pi$ stacked	4.54, 5.17
		Asp127	Attractive charge	5.17		Phe320	$\Pi$ - $\Pi$ stacked	5.84
		Tyr15	$\Pi$ - $\Pi$ T shaped	5.18, 5.96		His315	Alkyl, $\Pi$ -alkyl	4.48
		Phe80	Alkyl, $\Pi$ -alkyl	3.83		Phe320	Alkyl, $\Pi$ -alkyl	5.08
		Ala144	Alkyl, $\Pi$ -alkyl	4.08, 4.33		Met319	Alkyl, $\Pi$ -alkyl	4.59
		Ile10	Alkyl, $\Pi$ -alkyl	3.61		Pro316	Alkyl, $\Pi$ -alkyl	4.73, 5.11
						Ala244	Alkyl, $\Pi$ -alkyl	4.09, 4.53
						Ile234	Alkyl, $\Pi$ -alkyl	4.01, 5.02

Table 10 (continued)

Entry	CDK2 (PDB 6GUE)			DprE1 (PDB 4FDO)				
	Binding affinity (kcal/mol)	Interactions	Type of interaction	Distance	Binding affinity (kcal/mol)	Interactions	Type of interaction	Distance
<b>4h</b>	-9.6	Lys129	Conventional H bond	2.73	-8.3	Lys299	Conventional H bond	2.22
		Asp145	$\Pi$ -cation	4.98		Asp232	$\Pi$ -anion	3.53
		Lys89	$\Pi$ -anion	4.02		Phe362	$\Pi$ - $\Pi$ stacked	5.15
		Asp86	Attractive charge	3.75		Phe320	$\Pi$ - $\Pi$ stacked	5.78
		Glu81	C-H bond	3.25		His315	Alkyl, $\Pi$ -alkyl	4.47
		Glu12	C-H bond	3.68		Phe320	Alkyl, $\Pi$ -alkyl	5.0
		Ile10	$\Pi$ -sigma	3.78		Met319	Alkyl, $\Pi$ -alkyl	4.66
		Leu134	$\Pi$ -sigma	3.80		Pro316	Alkyl, $\Pi$ -alkyl	4.57, 5.11
		Ala144	Alkyl, $\Pi$ -alkyl	5.30		Ala244	Alkyl, $\Pi$ -alkyl	3.87, 4.54
		Val18	Alkyl, $\Pi$ -alkyl	5.10, 5.31		Ile234	Alkyl, $\Pi$ -alkyl	4.13, 4.89
		Ala31	Alkyl, $\Pi$ -alkyl	3.25, 3.70		Trp232	Alkyl, $\Pi$ -alkyl	4.45
		Leu83	Alkyl, $\Pi$ -alkyl	4.57				
		Leu134	Alkyl, $\Pi$ -alkyl	4.86				
		Val64	Alkyl, $\Pi$ -alkyl	5.40				

C-H carbon-hydrogen, H Hydrogen

**Supplementary Information** The online version contains supplementary material available at <https://doi.org/10.1007/s11164-024-05228-2>.

**Acknowledgements** We are thankful to Instrumentation Centre, Punyashlok Ahilyadevi Holkar Solapur University, Solapur, Council for Scientific and Industrial Research-Indian Institute of Chemical Technology (CSIR-IICT), Hyderabad and Sophisticated Analytical Instrumental Facility-Common Facility Center (SAIF-CFC), Shivaji University, Kolhapur for spectral analysis. The authors are thankful to Maratha Mandal's Central Research Laboratory, Belgaum for providing biological activities.

**Author contributions** PRK and SSR analyzed the data and wrote the main manuscript, SSR worked on software, SSD supervised the work, All authors reviewed the manuscript.

**Funding** This research work has not received any funds.

**Data availability** The data have been included in the article and supplementary information file.

## Declarations

**Conflict of interest** The authors declare no conflict of interest.

## References

1. R. Kaur, S. Chaudhary, K. Kumar, M.K. Gupta, R.K. Rawal, *Eur. J. Med. Chem.* **132**, 108 (2017)
2. L.E. Rodriguez, C.H. House, K.E. Smith, M.R. Roberts, M.P. Callahan, *Sci. Rep.* **9**, 9281 (2019)
3. N. Kerru, L. Gummidi, S. Maddila, K.K. Gangu, S.B. Jonnalagadda, *Molecules* **25**, 1909 (2020)
4. D. Zárate-Zárate, R. Aguilar, R.I. Hernández-Benitez, E.M. Labarrios, F. Delgado, J. Tamariz, *Tetrahedron* **71**, 6961 (2015)
5. E.K. Davison, J. Sperry, *J. Nat. Prod.* **80**, 3060 (2017)
6. W.Y. Fang, L. Ravindar, K.P. Rakesh, H.M. Manukumar, C.S. Shantharam, N.S. Alharbi, H.L. Qin, *Eur. J. Med. Chem.* **173**, 117 (2019)
7. B. Eftekhari-Sis, M. Zirak, A. Akbari, *Chem. Rev.* **113**, 2958 (2013)
8. Y. Ju, R.S. Varma, *J. Org. Chem.* **71**, 135 (2006)
9. P.D. Leeson, B. Springthorpe, *Nat. Rev. Drug Discov.* **6**, 881 (2007)
10. C. Lamberth, *Pest Manag. Sci.* **69**, 1106 (2013)
11. B.R. Smith, C.M. Eastman, J.T. Njardarson, *J. Med. Chem.* **57**, 9764 (2014)
12. J. Liu, J. Jiang, L. Zheng, Z.Q. Liu, *Adv. Synth. Catal.* **362**, 4876 (2020)
13. K. Paruch, Ł. Popiołek, A. Biernasiuk, A. Hordyjewska, A. Malm, M. Wujec, *Molecules* **25**, 5844 (2020)
14. S.B. Bakare, *Bull. Chem. Soc. Ethiop.* **35**, 449 (2021)
15. V. Alagarsamy, R. Giridhar, M.R. Yadav, *J. Pharm. Pharmacol.* **58**, 1249 (2010)
16. S. Nabil, S.N. Abd El-Rahman, S.S. Al-Jameel, A.M. Elsharif, *Biol. Pharm. Bull.* **41**, 1071 (2018)
17. M. Marinescu, *Antibiotics* **10**, 1002 (2021)
18. R. Bouley, M. Kumarasiri, Z. Peng, L.H. Otero, W. Song, M.A. Suckow, V.A. Schroeder, W.R. Wolter, E. Lastochkin, N.T. Antunes, H. Pi, S. Vakulenko, J.A. Hermoso, M. Chang, S. Mobashery, *J. Am. Chem. Soc.* **137**, 1738 (2015)
19. J. Jampilek, *Molecules* **24**, 3839 (2019)
20. W. Wang, L. Lei, Z. Liu, H. Wang, Q. Meng, *Molecules* **24**, 877 (2019)
21. S.H. Sharma, J.L. Pablo, M.S. Montesinos, A. Greka, C.R. Hopkins, *Bioorg. Med. Chem. Lett.* **29**, 155 (2019)
22. J. Liu, C. Wu, H. Jin, K. Du, H. Zheng, *J. Heterocycl. Chem.* **56**, 3088 (2019)
23. P. Herdewijn, *Antisense Nucleic Acid Drug Dev.* **10**, 297 (2000)
24. S.S. Gupta, S. Kumari, I. Kumar, U. Sharma, *Chem. Heterocycl. Compd. (New York)* **56**, 433 (2020)
25. K.P. Srivastava, I. Singh, A. Kumari, *Der Pharma Chem.* **6**, 119 (2014)
26. N.C. Desai, A.M. Dodiya, *Arab. J. Chem.* **9**, S379 (2016)

27. M.S. Praceka, S. Megantara, R. Maharani, M. Muchtaridi, J. Adv. Pharm. Technol. Res. **12**, 321 (2021)
28. R. Kakuchi, R. Ito, S. Nomura, H. Abroshan, K. Ninomiya, T. Ikai, K. Maeda, H.J. Kim, K. Takahashi, RSC Adv. **7**, 9423 (2017)
29. J.D. Patil, S.N. Korade, D.M. Pore, RSC Adv. **4**, 50449 (2014)
30. H.R. Safaei, M. Shekouhy, V. Shafiee, M. Davoodi, J. Mol. Liq. **180**, 139 (2013)
31. H. Zang, Q. Su, Y. Mo, B.W. Cheng, S. Jun, Ultrason. Sonochem. **17**, 749 (2010)
32. S.N. Korade, J.D. Patil, D.M. Pore, Monatsh. Chem. **147**, 2143 (2016)
33. J.D. Patil, S.A. Patil, D.M. Pore, RSC Adv. **5**, 21396 (2015)
34. V.I. Pârvulescu, C. Hardacre, Chem. Rev. **107**, 2615 (2007)
35. G. Bhasin, R. Srivastava, R. Singh, Org. Prep. Proc. Int. **49**, 370 (2017)
36. C. Maton, N. De Vos, C.V. Stevens, Chem. Soc. Rev. **42**, 5963 (2013)
37. R. Sheldon, ChemComm **1**, 2399 (2001)
38. B.J. Butler, J.B. Harper, New J. Chem. **39**, 213 (2015)
39. R.L. Vekariya, J. Mol. Liq. **227**, 44 (2017)
40. W.L. Wong, K.Y. Wong, Can. J. Chem. **90**, 1 (2012)
41. R.C. Cioc, E. Ruijter, R.V.A. Orru, Green Chem. **16**, 2958 (2014)
42. B.H. Rotstein, S. Zaretsky, V. Rai, A.K. Yudin, Chem. Rev. **114**, 8323 (2014)
43. A. Rahmati, N. Pashmforoush, Iran. Chem. Soc. **12**, 993 (2015)
44. J.D. Sunderhaus, S.F. Martin, Chem. Eur. J. **15**, 1300 (2009)
45. J.R. Resting, I.L. Tolderlund, A.F. Pedersen, M. Witt, J.W. Jaroszewski, D. Staerk, J. Nat. Prod. **72**, 312 (2009)
46. G.L. Lozano, H.B. Park, J.I. Bravo, E.A. Armstrong, J.M. Denu, E.V. Stabb, N.A. Broderick, J.M. Crawford, J. Handelsman, Appl. Environ. Microbiol. **85**, e03058 (2019)
47. M. Misra, S.K. Pandey, V.P. Pandey, J. Pandey, R. Tripathi, R.P. Tripathi, Bioorg. Med. Chem. **17**, 625 (2009)
48. M. Gangapuram, K. Redda, J. Heterocycl. Chem. **43**, 709 (2006)
49. K. Rao, K. Redda, F. Onayemi, H. Melles, J. Choi, J. Heterocycl. Chem. **32**, 307 (1995)
50. S. Petit, J. Nallet, M. Guillard, J. Dreux, R. Chermat, M. Poncelet, C. Bulach, P. Simon, C. Fontaine, M. Barthelmebs, J. Imbs, Eur. J. Med. Chem. **26**, 19 (1991)
51. Y. Zhou, V.E. Gregor, B.K. Ayida, G.C. Winters, Z. Sun, D. Murphy, G. Haley, D. Bailey, J.M. Froelich, S. Fish, S.E. Webber, T. Hermann, D. Wall, Bioorg. Med. Chem. Lett. **15**, 1206 (2007)
52. B. Ho, A.M. Crider, J.P. Stables, Eur. J. Med. Chem. **36**, 265 (2001)
53. S.S. Sajadikhah, M.T. Maghsoodlou, N. Hazeri, S.M. Habibi-Khorassani, S.J. Shams-Najafi, Monatsh. Chem. **143**, 939 (2012)
54. L. Wu, S. Yan, W. Wang, Y. Li, Res. Chem. Intermed. **46**, 4311 (2020)
55. S. Mohammadi, M. Abbasi, J. Chem. Res. **39**, 123 (2015)
56. M. Lashkari, M.T. Maghsoodlou, N. Hazeri, S.M. Habibi-Khorassani, S.S. Sajadikhah, R. Doost-mohamadi, Synth. Commun. **43**, 635 (2013)
57. J. Aboonajmi, M.T. Maghsoodlou, N. Hazeri, M. Lashkari, M. Kangani, Res. Chem. Intermed. **41**, 8057 (2015)
58. D. Dogra, R. Bharti, R. Sharma, Orbital **12**, 232 (2020)
59. S. Geetha, A. Thangamani, R. Valliappan, S. Vedanayaki, A. Ganapathi, Chem. Data Collect. **30**, 100565 (2020)
60. A.T. Khan, M. Lal, M.M. Khan, Tetrahedron Lett. **51**, 4419 (2010)
61. A. Mulik, P. Hegade, D. Patil, G. Mulik, S. Salunkhe, M. Deshmukh, Res. Chem. Intermed. **43**, 729 (2016)
62. S. Sardar, C.D. Wilfred, L.J. Marc, AIP Conf. Proc. **1787**, 030010 (2016)
63. S.A. Hattarki, C. Bogar, K. Bhat, Int. J. Pharm. Res. Health Sci. **8**, 3220 (2020)
64. P. Mandroli, A. Prabhakar, K. Bhat, S. Krishnamurthy, C. Bogar, Ayu **40**, 192 (2019)
65. S. Cho, H.S. Lee, S. Franzblau, Methods Mol. Biol. **1285**, 281 (2015)
66. M.C.S. Lourenço, M.V.N. de Souza, A.C. Pinheiro, M.L. de Ferreira, R.S.B. Gonçalves, T.M. Cristina Nogueira, M.A. Peralta, ARKIVOC **15**, 181 (2007)
67. E.J. Walsh, J. Chem. Educ. **74**, 3 (1997)
68. Dassault Systèmes, (2020).
69. N.M. O'boyle, M. Banck, C.A. James, C. Morley, T. Vandermeersch, G.R. Hutchison, J. Cheminform. **3**, 1 (2011)

70. V.K. Bagal, S.S. Rathod, M.M. Mulla, S.C. Pawar, P.B. Choudhari, V.T. Pawar, D.V. Mahuli, *Nat. Prod. Res.* **37**, 1 (2023)
71. A. Daina, O. Michielin, V. Zoete, *Sci. Rep.* **7**, 42717 (2017)
72. D.E.V. Pires, T.L. Blundell, D.B. Ascher, *J. Med. Chem.* **58**, 4066 (2015)
73. S. Rochlani, M. Bhatia, S. Rathod, P. Choudhari, and R. Dhavale, *Nat. Prod. Res.* **1** (2023).
74. J. T. Kilbile, Y. Tamboli, S. A. Ansari, S. S. Rathod, P. B. Choudhari, H. Alkahtani, and S. B. Sankal, *Polycycl. Aromat. Compd.* **1** (2023).
75. S. Rathod, S. Dey, S. Pawar, R. Dhavale, P. Choudhari, E. Rajakumara, D. Mahuli, D. Bhagwat, Y. Tamboli, P. Sankpal, S. Mali, and H. More, *J. Biomol. Struct. Dyn.* **1** (2023).
76. F. Neese, *Wiley Interdiscip. Rev. Comput. Mol. Sci.* **2**, 73 (2012)
77. H.D. Snyder, T.G. Kucukkal, *J. Chem. Educ.* **98**, 1335 (2021)
78. V. Puthanveedu, K. Muraleedharan, *Struct. Chem.* **33**, 1423 (2022)
79. S. Choudhari, S. K. Patil, and S. Rathod, *J. Biomol. Struct. Dyn.* **1** (2023).
80. S. Rathod, D. Bhande, S. Pawar, K. Gumphalwad, P. Choudhari, and H. More, *Chem. Afr.* (2023).
81. H.M. Berman, J. Westbrook, Z. Feng, G. Gilliland, T.N. Bhat, H. Weissig, I.N. Shindyalov, P.E. Bourne, *Nucleic Acids Res.* **28**, 235 (2000)
82. R. D. Bakale, P. S. Phatak, S. S. Rathod, P. B. Choudhari, E. M. Rekha, D. Sriram, R. S. Kulkarni, and K. P. Haval, *J. Biomol. Struct. Dyn.* **1** (2023).
83. J. Eberhardt, D. Santos-Martins, A.F. Tillack, S. Forli, *J. Chem. Inf. Model.* **61**, 3891 (2021)
84. S. Rathod, P. Chavan, D. Mahuli, S. Rochlani, S. Shinde, S. Pawar, P. Choudhari, R. Dhavale, P. Mudalkar, F. Tamboli, *J. Mol. Model.* **29**, 1 (2023)
85. S.Y. Salunkhe, R.P. Gurav, S.S. Rathod, P.B. Choudhari, T.P. Yadav, S.B. Wakshe, P.V. Anbhule, G.B. Kolekar, *J. Mol. Struct.* **1301**, 137288 (2024)
86. S. Rathod, K. Shinde, J. Porlekar, P. Choudhari, R. Dhavale, D. Mahuli, Y. Tamboli, M. Bhatia, K.P. Haval, A.G. Al-Sehemi, M. Pannipara, *ACS Omega* **8**, 391 (2022)
87. P. Swami, S. Rathod, P. Choudhari, D. Patil, A. Patravale, Y. Nalwar, S. Sankpal, S. Hangirgekar, *J. Mol. Struct.* **1292**, 136079 (2023)
88. S. Dey, S. Rathod, K. Gumphalwad, N. Yadav, P. Choudhari, E. Rajakumara, R. Dhavale, and D. Mahuli, *J. Biomol. Struct. Dyn.* **1** (2023).
89. H. Eshghi, A. Khojastehzhad, F. Moeinpour, M. Bakavoli, S.M. Seyedi, M. Abbasi, *RSC Adv.* **4**, 39782 (2014)
90. M. Abbasi, *RSC Adv.* **5**, 67405 (2015)
91. R. Jahanshahi, B. Akhlaghinia, *New J. Chem.* **41**, 7203 (2017)
92. N.R. Agrawal, S.P. Bahekar, P.B. Sarode, S.S. Zade, H.S. Chandak, *RSC Adv.* **5**, 47053 (2015)
93. R. Ramachandran, S. Jayanthi, Y.T. Jeong, *Tetrahedron* **68**, 363 (2012)
94. G.V. Ramin, S. Hajar, *C. R. Chim.* **16**, 1047 (2013)
95. S.S. Sajadikhah, N. Hazeri, M. Taher Maghsoodlou, M. Habibi-Khorassani, A. Beigbabaei, M. Lashkari, *J. Chem. Res.* **36**, 463 (2012)
96. M. Zarei, S.S. Sajadikhah, *Res. Chem. Intermed.* **42**, 7005 (2016)
97. D.D. Gadge, P.S. Kulkarni, *J. Heterocycl. Chem.* **59**, 1320 (2022)
98. C.A. Lipinski, *Drug Discov. Today Technol.* **1**, 337 (2004)
99. C.A. Lipinski, B.W. Dominy, P.J. Feeney, *Adv. Drug Deliv. Rev.* **23**, 3 (1997)
100. C.A. Lipinski, F. Lombardo, B.W. Dominy, P.J. Feeney, *Adv. Drug Deliv. Rev.* **23**, (2001)
101. D.F. Veber, S.R. Johnson, H.Y. Cheng, B.R. Smith, K.W. Ward, K.D. Kopple, *J. Med. Chem.* **45**, 2615 (2002)
102. J.X. Mu, Y.X. Shi, M.Y. Yang, Z.H. Sun, X.H. Liu, B.J. Li, N.B. Sun, *Molecules* **21**, 68 (2016)
103. P. Patil, P. Patil, P. Dandge, P. Bansode, B. Kumbhar, W. Chandane, S. Rathod, P. Choudhari, S. Khot, N. Valekar, D. Pore, G. Rashinkar, *J. Mol. Struct.* **1301**, 137202 (2024)
104. E.B. Elkaeed, R.G. Yousef, H. Elkady, I.M.M. Gobaara, B.A. Alsouk, D.Z. Husein, I.M. Ibrahim, A.M. Metwaly, I.H. Eissa, *Molecules* **27**, 4606 (2022)
105. P.K. Patial, D.S. Cannoo, *Nat. Prod. Res.* **35**, 4611 (2021)
106. M.A. Mumit, T.K. Pal, M.A. Alam, M.A.A.A.A. Islam, S. Paul, M.C. Sheikh, *J. Mol. Struct.* **1220**, 128715 (2020)
107. R.D. Bakale, S.M. Sulakhe, S.L. Kasare, B.P. Sathe, S.S. Rathod, P.B. Choudhari, E. Madhu Rekha, D. Sriram, K.P. Haval, *Bioorg. Med. Chem. Lett.* **97**, 129551 (2023)
108. A. Das, A. Das, B.K. Banik, *J. Indian Chem. Soc.* **98**, 100005 (2021)
109. A. Das, B.K. Banik, *Green Approaches in Medicinal Chemistry for Sustainable Drug Design* (Elsevier, Amsterdam, 2020), pp.921–964

110. D.M. Kara, I.J. Smallman, J.J. Hudson, B.E. Sauer, M.R. Tarbutt, E.A. Hinds, *New J. Phys.* **14**, 103051 (2012)
111. M.N. Tahir, M. Khalid, A. Islam, S.M. Ali Mashhadi, A.A.C. Braga, *J. Mol. Struct.* **1127**, 766 (2017)
112. A.R. Pasha, M. Khalid, Z. Shafiq, M.U. Khan, M.M. Naseer, M.N. Tahir, R. Hussain, A.A.C. Braga, R. Jawaria, *J. Mol. Struct.* **1230**, 129852 (2021)
113. G. Mustafa, I. Shafiq, Q.U.A. Shaikh, A. Mustafa, R. Zahid, F. Rasool, M.A. Asghar, R. Baby, S.M. Alshehri, M. Haroon, *ACS Omega* **8**, 22673 (2023)
114. A. Ali, M. Khalid, K.P. Marrugo, G.M. Kamal, M. Saleem, M.U. Khan, O. Concepción, A.F. de la Torre, *J. Mol. Struct.* **1207**, 127838 (2020)
115. M. Khalid, H.M. Lodhi, M.U. Khan, M. Imran, *RSC Adv.* **11**, 14237 (2021)
116. M. Riaz, F. Jan, A. Khan, A. Ullah, H. Haq, A.F. AlAsmari, M. Alharbi, F. Alasmari, MominKhan, *Arab. J. Chem.* **16**, 105259 (2023)
117. C. Weetman, S. Inoue, *ChemCatChem* **10**, 4213 (2018)
118. P. Wu, P. Du, H. Zhang, C. Cai, *J. Phys. Chem. C* **116**, 20472 (2012)
119. S.K. Seth, G.C. Maity, T. Kar, *J. Mol. Struct.* **1000**, 120 (2011)
120. S.K. Seth, N.C. Saha, S. Ghosh, T. Kar, *Chem. Phys. Lett.* **506**, 309 (2011)
121. S.K. Seth, S. Banerjee, T. Kar, *J. Mol. Struct.* **965**, 45 (2010)

**Publisher's Note** Springer Nature remains neutral with regard to jurisdictional claims in published maps and institutional affiliations.

Springer Nature or its licensor (e.g. a society or other partner) holds exclusive rights to this article under a publishing agreement with the author(s) or other rightsholder(s); author self-archiving of the accepted manuscript version of this article is solely governed by the terms of such publishing agreement and applicable law.

## Authors and Affiliations

**Pravin R. Kharade<sup>1,5</sup> · Uttam B. Chougale<sup>1,5</sup> · Dipak S. Gaikwad<sup>2</sup> · Satish S. Kadam<sup>2</sup> · Kiran N. Patil<sup>3</sup> · Sanket S. Rathod<sup>4</sup> · Prafulla B. Choudhari<sup>4</sup> · Savita S. Desai<sup>5</sup>**

✉ Pravin R. Kharade  
pravinkharade03@gmail.com

✉ Savita S. Desai  
savitadesai2010@gmail.com

<sup>1</sup> Department of Chemistry, Karmaveer Hire Arts, Science, Commerce and Education College, Gargoti, Maharashtra 416209, India

<sup>2</sup> Department of Chemistry, Vivekanand College (Autonomous), Kolhapur, Maharashtra 416003, India

<sup>3</sup> Department of Chemistry, Dr. Ghali College, Gadhinglaj, Maharashtra 416502, India

<sup>4</sup> Department of Pharmaceutical Chemistry, Bharati Vidyapeeth College of Pharmacy, Kolhapur, Maharashtra 416013, India

<sup>5</sup> Research Laboratory in Heterocyclic Chemistry, Devchand College, Arjunnagar, Maharashtra 416216, India